

Added Mass of High-Altitude Balloons

W. J. Anderson* and Gourang Shah†

A92-11034

Dept. of Aerospace Engineering, Univ. of Michigan, Ann Arbor MI 48109.

August 13, 1991

Abstract

A body immersed in a fluid displaces an amount of fluid equal to its volume. When such a body is accelerated, pressures are generated which affect the fluid field to infinity. This creates kinetic energy in the fluid. One can define an effective mass of fluid accelerating with the body; this is called the "added" mass. Historically, the calculation of added mass was in the province of hydrodynamics.

The present study uses the theory of acoustics to develop the added mass for several rigid, immersed bodies. A numerical solution is used, based on boundary elements. The classical cases of a circular disk and a sphere are used to determine the mesh fineness required for engineering accuracy. A family of three Smalley-shaped balloons (zero circumferential stress in the film) are then considered, for different inflation ratios. Incompressibility of the fluid is assumed, therefore the added masses are identical in spirit with those from hydrodynamics. Compressibility is not important for rigid body dynamics of balloons; however compressibility effects can be included for other bodies, if needed.

Results show that the pear-shaped balloons behave in an intermediate way between spheres and cylinders, as expected. Both vertical and horizontal accelerations are considered. The values for added masses will allow better dynamics studies of high-altitude balloons.

A major feature of the paper is to demonstrate the feasibility of calculating added masses for arbitrarily-shaped bodies using acoustics. This should become a standard working tool for studies of immersed bodies such as balloons, parachutes, and submarines.

Nomenclature

C	= coupling matrix
F_S	= structural force
F_A	= acoustic load vector
$[H]$	= fluid matrix
k	= wave number
$[K]$	= stiffness matrix
$[M]$	= mass matrix
$\{Q\}$	= potential (jump of pressure) vector
S_1	= surface on which pressures are specified
S_2	= surface on which velocities are specified
$\{U\}$	= displacement vector
ρ	= fluid density
w	= frequency, in rad/sec

Superscript

T	= transpose
-1	= inverse

Subscript

A	= added mass
S	= structural

1. Introduction

Much recent progress in the area of numerical modeling of coupled acoustics/structures has been made.^[1,2,3] One major software package uses boundary elements for the fluid discretization.^[4] As a side-capability, this modeling procedure can determine the added mass due to rigid-body structural accelerations. The effect of the pressure field is to retard the acceleration of the body, and the resulting added mass of the body can then be deduced. This capability has not existed before, and promises to aid the study of bodies such as balloons, parachutes and submarines where the bodies carry a large amount of fluid with them.

*Professor of Aerospace Engineering, member AIAA.

†Graduate Student, Aerospace Engineering.

Copyright ©1991 by William J. Anderson.

Published by the American Institute of Aeronautics and Astronautics, Inc. with permission.

2. Eigenvalue equations

This study is based on a solution of the Helmholtz equation. One can solve the acoustic problem either by a potential field solution or by a pressure field solution. The present approach is to consider the pressure field as the primary variable and to cast boundary conditions into functions of pressure. The Helmholtz equation is:

$$\nabla^2 p + k^2 p = 0 \quad (1)$$

and the associated boundary conditions are:

$$p = \bar{p} \quad (\text{on surface } S_1) \quad (2)$$

$$v_r = \bar{v}_n \quad (\text{on surface } S_2) \quad (3)$$

In addition, one has the Sommerfeld radiation condition for unbounded domains:

$$r \xrightarrow{\text{lim}} \infty \quad r \left(\frac{\partial p}{\partial n} + ikp \right) = 0 \quad (4)$$

The solution to these equations has been carried out for various shaped boundary elements in a commercial computer program, SYSNOISE. The acoustic disturbance for quadrilateral and triangular elements will be used here. When the field pressures for such boundary elements are found, they exist on both sides of the element. The result is, that for hollow bodies, the boundary elements model the fluid presence on both the interior and exterior of the body. (For the balloon, the presence of the interior air is spurious and its contribution to the added mass must be removed.)

After the fluid field is modeled by boundary elements, the structure is modeled by conventional finite elements. The rigid body modes of the structure are found and modal coordinates are used to describe the displacements of the structure.

One then solves the eigenvalue problem describing coupled oscillations of the structure and fluid field, and infers the mass of the fluid. The system of coupled equations developed for the structure and the fluid are:

$$\begin{bmatrix} K_S - \omega^2 M_S & C^T \\ C & \frac{H(k)}{\rho_f \omega^2} \end{bmatrix} \begin{Bmatrix} U \\ Q \end{Bmatrix} = \begin{Bmatrix} F_S \\ F_A \end{Bmatrix} \quad (5)$$

The virtual mass matrix results from elimination of Q from Eqn. 5 and assuming free vibration (zero force on **RIIS**).

$$\{Q\} = -\rho_F \omega^2 [H(k)]^{-1} [C] \{U\} \quad (6)$$

This is substituted into the upper vector equation in Eqn. 5 to obtain:

$$\left([K_S] - \omega^2 ([M_S] + [M_A(k)]) \right) \{U\} = \{0\} \quad (7)$$

where

$$[M_A(k)] = \rho_F [C]^T [H(k)]^{-1} [C] \quad (8)$$

is the added mass matrix. To this point, the added mass is frequency dependent, so that the eigenproblem 7 is not a conventional algebraic eigenvalue problem. We will now, however, assume that the fluid is incompressible. This means that the wave number k is set to zero. The added mass can be shown to be real in this case. Equation 7 can then be solved using subspace iteration (for example).

The mass matrix $[M_A]$ is a full symmetric matrix due to the use of the boundary element model for the fluid. The banded character of the original structural mass matrix is therefore of little value.

Finally, there has been conflicting use of the words "added mass" and "virtual mass" in the literature. Hydrodynamicists^[5] have used added mass to describe the fluid contribution only, and virtual mass to refer to the total mass of the structure and fluid. Aeroelasticians^[6] have used virtual mass to apply to the fluid contribution only. In this paper, the authors will use the term added mass for the fluid contribution only. The term virtual mass will be avoided because it has been compromised by the two usages.

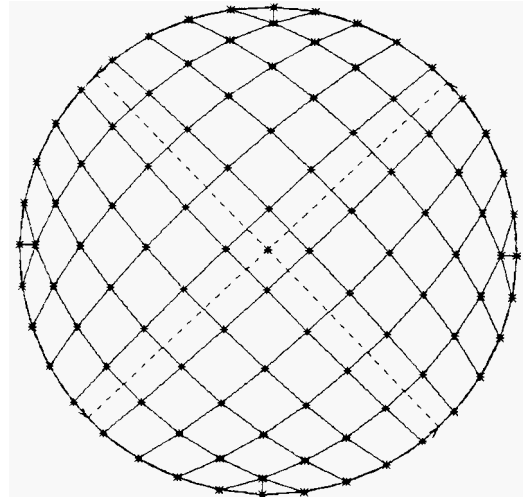


Figure 1: Boundary element mesh for circular disk.

3. Preliminary studies (classical)

To develop some feeling for the added mass calculations, it is helpful to repeat some classical cases. This will also aid in deciding on mesh refinement needed.

The first case studied is a rigid, circular disk of one meter radius, moving normal to its plane in air. This case is difficult numerically because of the sharp edges of the disk. Care must be taken to set the pressure jump across this cut edge to zero (reminiscent of the Kutta-Joukowski condition for lifting airfoils). The textbook solution for the added mass is:^[5]

$$M_A = 2.6667 \text{ kg} \quad (9)$$

Five mesh densities were used to study convergence. A mesh with 85 elements is shown in Fig. 1. The nodes are placed on the reference diameter, therefore the disk area is underestimated.

The results are given in Fig. 2. The number of boundary elements is used as a measure of mesh refinement, rather than the number of nodes. When one uses 9 ele-

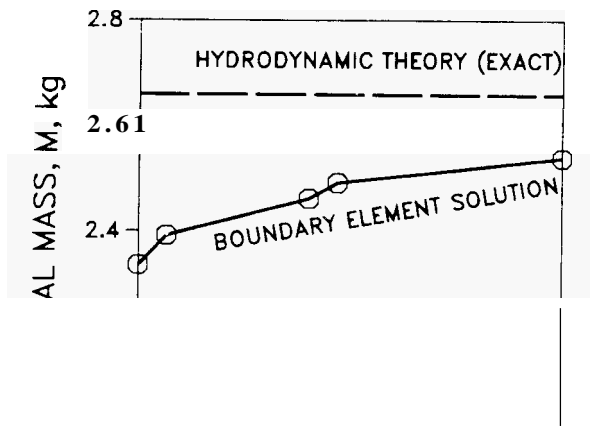


Figure 2: Virtual mass of circular disk.

ments per side, the error in the added mass is less than 7%. The error consists of two major parts: that due to the area underestimation, and that due to the small number of elements modeling a continuum.

The second case studied is a sphere. This can be solved in closed form^[5] and the added mass is found to be one-half the displaced fluid mass. This holds for accelerations in all directions, of course. The sphere has no “cut edges,” and there is no need to apply side conditions on pressure jump at its “boundaries.” The mesh is shown in Fig. 3.

The nodal points for the boundary elements are placed on the reference diameter. The boundary elements form a faceted surface which lies inside the reference sphere, and hence displaces a smaller amount

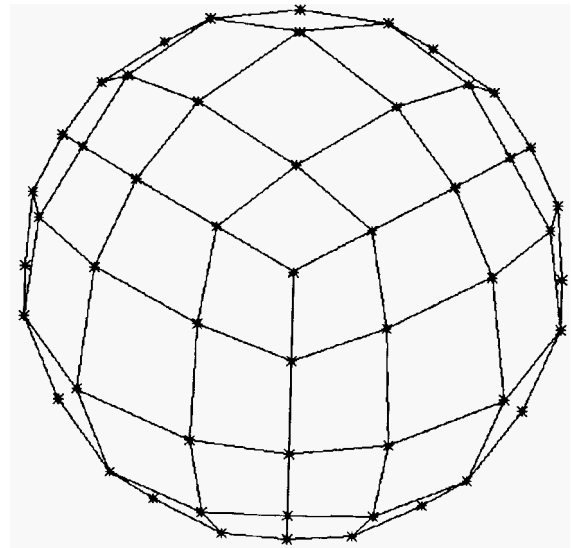


Figure 3: Mesh for sphere with hidden line removal.

of fluid than the reference sphere. (See Fig. 4.) As a result, the “raw” answer obtained for added mass is for a smaller body than the reference sphere. It was

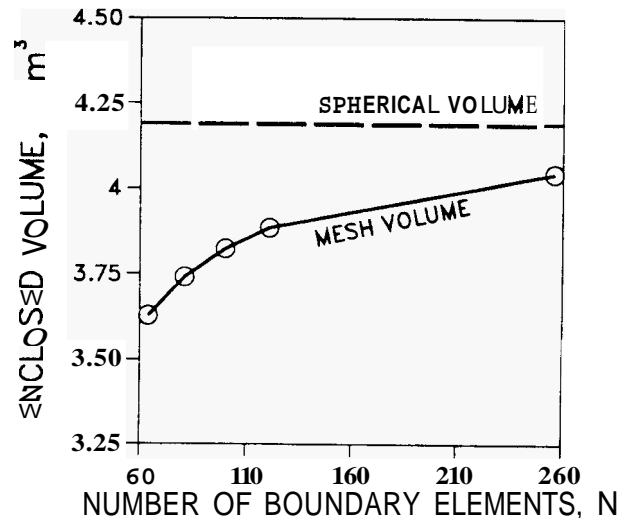


Figure 4: Volume enclosed within faceted sphere.

decided to correct the inertia coefficient to account for the actual amount of displaced volume. This reduces the convergence issue to one involving the coarseness of the mesh, and removes the question of the reference volume. Convergence studies (below) done for the balloon shapes show better convergence with such volume correction.

The use of volume-correction is also needed for a sec-

ond reason. The boundary element solution for the sphere includes not only the outer fluid field, but also the (same) fluid within the sphere. This internal air mass is extraneous in our case since actual balloons carry helium, not air. For dynamics calculations, the internal mass of helium must be added in at some point. The inertia coefficient calculation becomes sensitive to volume error if the volume correction is not done.

One acoustic study was done for the sphere using SYSNOISE. This was for a mesh of 96 boundary elements. The volume-corrected inertia factor was found to be 0.505, which has error of only +0.8%. This shows the effectiveness of the volume correction, since the displaced volume has only converged to within -8% of the smooth sphere.

4. Balloon studies

A family of balloons of the Smalley type (zero circumferential stress) will be considered. Three balloon inflation ratios will be considered—partial, half and full inflation. Rand^[7] has provided a procedure to size the balloons for given inflation ratios. This procedure will be used to lay out the balloon shape. The balloon cross-sections are shown in Fig. 5. They correspond to inflation fractions of 0.0031, 0.113 and 1.000 from top to bottom, respectively.

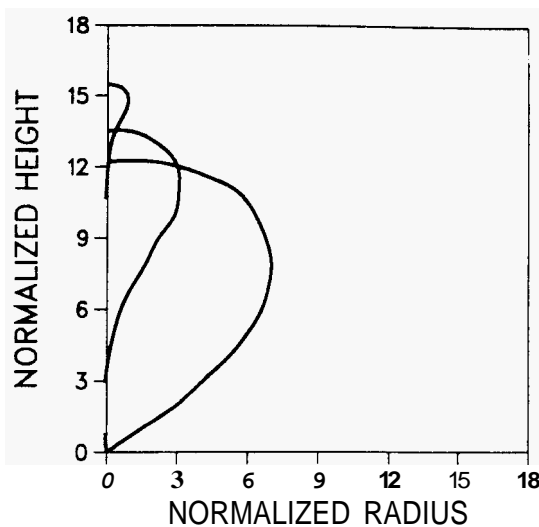


Figure 5: Cross-sections of balloons for varying inflation.^[7]

The balloon mesh was constructed by creating a 1/8 section of the balloon and then replicating it 8 times with the preprocessor I-DEAS. The completed model is

axisymmetric, that is, no attempt was made to account for the scalloped nature of the segments as the film bulges from the load tapes.

The fully inflated (float) balloon case has been studied more intensively than the others, in order to resolve the mesh density issue. Figures 6, 7 and 8 show the three mesh densities. From the experience with the sphere, one would expect this more complicated body to be adequately modeled with 256 elements, and rather accurately modeled with 432 elements.

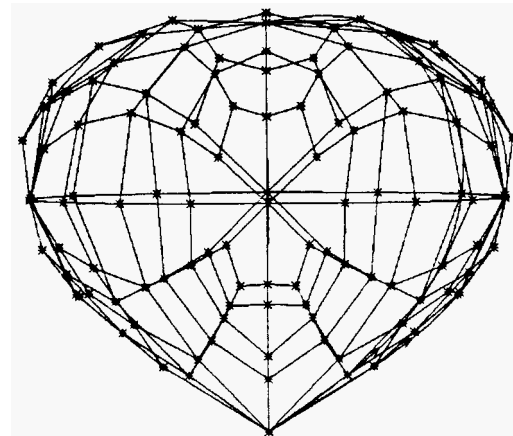


Figure 6: Coarse mesh for balloon at float.

The results for added mass in the axial and lateral directions are given in Table 1. The difference between the fine and the medium mesh is 2.8% and 0.5% for the axial and lateral cases, respectively. Convergence is from above, therefore the true values for added mass will be slightly lower than the fine mesh result. For engineering purposes, it appears that the medium mesh will be sufficient to study the family of balloons.

Results for a family of partially-inflated balloons are plotted in Fig. 9. The full balloon has one characteristic of the flat disk, e. g. the axial inertia is higher than the lateral. The inertial coefficients range from 0.42 to 0.64, depending on the inflation and the orientation of acceleration. More points at intermediate inflation are currently being calculated.

To date there have been limited experimental results to compare with this theory. The NASA/GSFC Wallops Flight Facility has flown tethered small-scale balloons and has measured inertia coefficients for vertical acceleration of approximately 0.55.^[8] In the past, re-

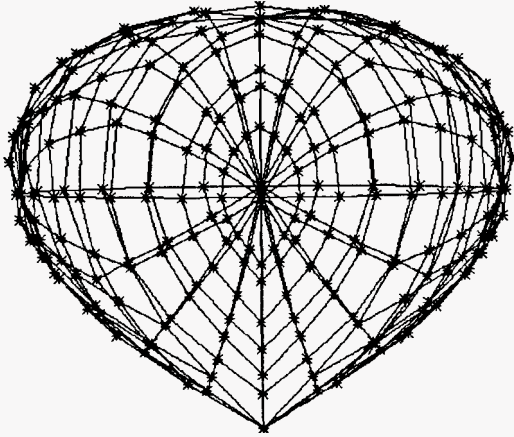


Figure 7: Medium mesh for balloon at float.

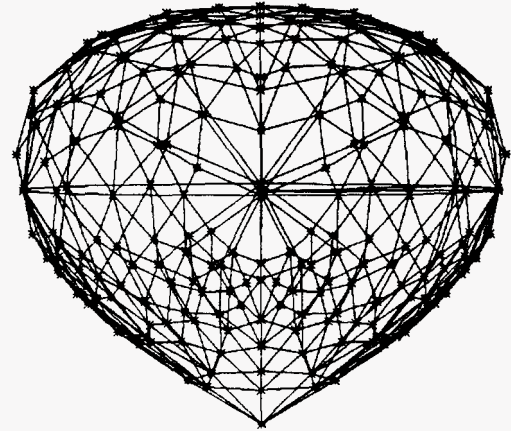


Figure 8: Fine mesh for balloon at float.

Table 1: Inertia coefficients for balloons

Mesh	Coarse	Medium	Fine
Elements	112	256	432
Nodes	114	226	218
Enclosed Volume	1.6416	1.7152	1.7262
Raw Axial Inertia	0.540	0.599	0.592
Raw Lateral Inertia	0.337	0.380	0.387
Corrected Ax. Inert.	0.673	0.663	0.645
Corrected Lat. Inert.	0.453	0.435	0.433
SYSNOISE CPU Time	6 sec	10 sec	16 sec

searchers often applied the value of 0.5 for spheres to the study of high-altitude balloon.^[9] The current values will allow much greater accuracy in dynamic calculations.

5. Computational details

Three software packages were used for this study. The I-DEAS preprocessor was used to generate the mesh. MSC/NASTRAN was used to generate the rigid body mode information. SYSNOISE was used for the numerical acoustics. An alternate approach would have been to use ANSYS for the generation of the mesh and modal information and SYSNOISE for the acoustic analysis. (ANSYS and SYSNOISE are tuned to work with each other.)

The computers used were Apollo 3500 workstations,

on The University of Michigan Computer Aided Engineering Network (CAEN). There are more than 100 Apollo machines on the University ring network. The computer time expended was far greater for mesh generation and modal analysis than for the acoustic solution. SYSNOISE CPU times are give in Table 1.

6. Conclusions

A numerical method has been used to find added mass for high altitude balloons. The method will be useful for other bodies immersed in fluids, whether planar or solid bodies. One must account for the presence of sharp edges (and the need for a zero pressure jump across the edge) and the presence of fictitious interior fluid in solid bodies.

The specific inertia coefficients obtained for high-altitude balloons will help in developing flight simulation codes that model dynamic balloon behavior. Common sources of excitation include ballast drops which cause axial acceleration and side winds that cause lateral accelerations. The inertia coefficients obtained range from 0.43 to 0.64 depending on inflation and direction of acceleration. These new values should replace the classical value of 0.5 for a sphere, which has been used in many calculations to date.

Acknowledgments

The computer software used in this paper was made available through University programs from Numerical Integration Technologies (SYSNOISE), Structural Dy-

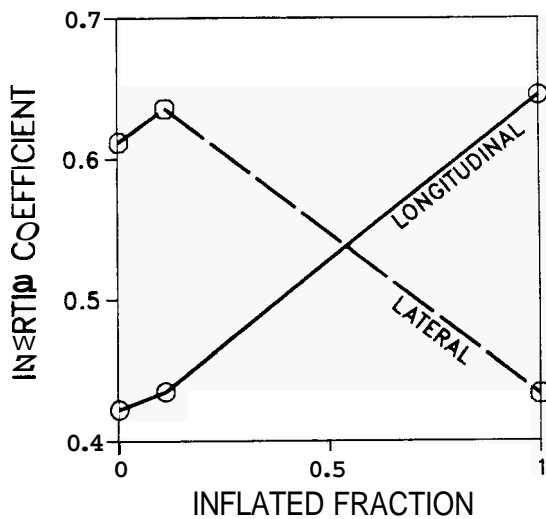


Figure 9: Inertia coefficients for partially-filled balloons.

namics Research Corp. (I-DEAS), and The MacNeal-Schwendler Corp. (MSC/NASTRAN). The use of these programs is greatly appreciated. Technical comments have been received by Jean-Pierre Coyette of Numerical Integration Technologies and Greg Sorter of Automated Analysis Corporation.

REFERENCES

1. Zienkiewicz, O. C., Kelly, D. W., and Bettess, P., "The coupling of the finite element method and boundary solution procedures," *International Journal for Numerical Methods in Engineering*, Vol. **11**, 1977 pp. 355-375.
2. Huang, H, "Helmholtz integral equations for fluid-structure interaction," *Advances in Fluid-Structure Interaction*, ASME, AMD Vol. **64**, New York, 1984, pp. 19-38.
3. Ousset, Y. and Sayhi, M. N., "Added mass computations by integral equation methods," *International Journal for Numerical Methods in Engineering*, Vol **19**, 1983, pp. 1355-1373.
4. SYSNOISE Theoretical Manual, Version 4.3, Numerical Integration Technology, Heverlee, Belgium, July, 1990.
5. Lamb, Sir Horace, "Hydrodynamics," 6th Edition, Dover Publications, New York, 1945, pp. 123,124.
6. Bisplinghoff, R. L., Ashley, H., and Halfman, R. L., "Aeroelasticity," Addison-Wesley Publishing Company,

Reading MA, 1955, p. 200.

7. Rand, James, "Shape and Stress of an Ascending Balloon," Winzen International, Inc., San Antonio TX 78213, Report No. WII-9936-FR-01, June, 1987.

8. Robbins, E., and Martone, M., "Determination of Balloon Gas Mass and Revised Estimates of Drag and Virtual Mass Coefficients," COSPAR XXVII Plenary Meeting and Associated Activities, The Hague, The Netherlands, July 1990.

9. Anderson, William J., and Taback, Israel, "Oscillations of High-Altitude Balloons," *Journal of Aircraft*, in press, 1991.